IOP Conf. Series: Materials Science and Engineering **342** (2018) 012063 doi:10.1088/1757-899X/342/1/012063

Preparation and characterization of 6-layered functionally graded nickel-alumina (Ni-Al_2O_3) composites

M I A Latiff[1], D M Nuruzzaman[2], S Basri[3], N M Ismail[4], S N S Jamaludin[5] and F F Kamaruzaman[4]

[1,2,4] Faculty of Manufacturing Engineering, University Malaysia Pahang, 26600 Pekan, Pahang Darul Makmur, Malaysia
[3] Office of the Assistant Vice Chancellor (Development), University Malaysia Kelantan, 16100 Kota Bharu, Kelantan Darul Naim, Malaysia
[5] Faculty of Engineering, DRB-HICOM University of Automotive Malaysia, 26607 Pekan, Pahang Darul Makmur, Malaysia

E-mail: dewan052005@yahoo.com

Abstract. The present research study deals with the preparation of 6-layered functionally graded (FG) metal-ceramic composite materials through powder metallurgy technique. Using a cylindrical die-punch set made of steel, the nickel-alumina (Ni-Al_2O_3) graded composite structure was fabricated. The samples consist of four gradual inter layers of varied nickel composition (80wt.%, 60wt.%, 40wt.%, 20wt.%) sandwiched with pure Ni and Al_2O_3 powders at the ends (100wt.% and 0wt.% nickel) were fabricated under 30 ton compaction load using a hydraulic press. After that, two-step sintering was carried out at sintering temperature 1200°C and soaking time 3 hours was maintained in a tube furnace. The properties of the prepared samples were characterized by radial shrinkage, optical microscopy and hardness testing. Results showed that larger shrinkage occurred within the ceramic phase which proves that more porosities were eliminated in the ceramic rich layers. From the microstructural analysis, it was observed that alumina particles are almost uniformly distributed in nickel matrix, so as nickel particles in the ceramic matrix of alumina-dominant layers. From interfacial analyses, it was observed that a smooth transition in microstructure from one layer to the next confirms a good interfacial solid state bonding between metal-ceramic constituents and good compaction process. On the other hand, microhardness test results suggest that there might be increasing percentage of porosities in the graded structure as the ceramic content rises.

1. Introduction

At present, the demand for new materials is growing rapidly for advanced engineering applications. A material of single composition with uniform structure may not satisfy all the requirements simultaneously. Functionally graded material (FGM) is a class of advanced composite which combines both the good properties of pure metal and pure ceramic beside possesses multifunctional properties to accommodate its applications in extreme environments. FGM is a combination of two or more material constituents, gradually changing in composition and properties from one side to the other along the thickness. The graded nature which may be continuous or stepwise (layer by layer) improves the bonding between material constituents and eliminates the stress at the interface. In processing of these graded composite materials various fabrication methods are available namely, thermal spraying, chemical vapour deposition, powder metallurgy and centrifugal casting [1-5]. In recent years, powder metallurgy method is widely used to produce the functional gradients in order to meet the requirements [6,7]. In processing the graded composite system, sintering is the most

challenging step. Cracks or defects are very common within the structure during the sintering of multi-layered composite systems due to the mismatch in thermal expansion of the graded layers [8].

Research efforts were carried out in order to investigate the properties of the functionally graded materials of different combinations theoretically and experimentally [9-13]. The obtained results revealed that mechanical responses of the graded composite systems remarkably influenced by material composition, number of layers, sintering temperature, compaction load etc. Mechanical responses of the graded aluminium composites were investigated at the outer, middle and inner regions [14]. The outer regions of the composites showed higher hardness as compared to the middle or inner regions. Moreover, outer region of the composites exhibited higher strength than the inner region. The properties of hydroxyapatite-titanium graded composite structures fabricated under different sintering atmospheres were investigated [15]. From the obtained results it was noticed that the graded structures were significantly influenced by different sintering atmospheres. Stainless steel graded parts were fabricated using laser melting deposition technique [16]. In this investigation, microstructure of different composition gradient, microhardness along the gradient direction were analysed. The obtained results revealed that good bonding was achieved between the deposited material and the substrate.

The design of the graded structure is controlled in terms of the geometrical aspects, such as number of layers and the layer thickness with systematically varied composition. The material variables such as chemical composition of powder compact, particle size distribution and particle shape are also considered as these factors influence the compressibility and sinterability of the fabrication process. In addition, processing parameters such as sintering time, sintering temperature, heating and cooling rate, sintering atmosphere are also important in order to prepare successful specimens. Considering these factors, in this research, Ni-Al_2O_3 functionally graded composite system was chosen since the properties of Ni and Al_2O_3 precursors are well characterized in a wide temperature range [9]. Six-layered nickel-alumina (Ni-Al_2O_3) functionally graded composite specimens were prepared using powder metallurgy and two-step pressureless sintering technique using argon atmosphere. Specimens were designed to have pure constituents (Ni and Al_2O_3) sandwiched the gradual layers which changing uniformly in composition by 20wt.% Ni across each layer. This configuration ultimately formed a six-layered FGM system. In order to characterize and to measure the quality of the graded composite, it is important to analyse the shrinkage, microhardness and microstructural properties. Considering all these issues, the nickel-alumina functionally graded composite specimens were analysed for shrinkage and microhardness. Microstructural and interfacial characteristics were also analysed in this study.

2. Experimental

In processing the Ni-Al_2O_3 functionally graded system, factors such as particle size and shape, layer thickness and number of layers were considered. Ni possesses high ductility and stiffness while being resistive towards corrosive environments. Al_2O_3 on the contrary is low in density and electrical resistivity while having high hardness and stiffness. Besides, low coefficient of thermal expansion (CTE) of Al_2O_3, at the same time having high melting point and highly resistant towards corrosion makes it suitable for combined with metals and applicable as super heat resistance materials [9]. Powder metallurgy (PM) technique was chosen for this research because of the simplicity of the process and it is applicable to a wide range of material combinations including Ni-Al_2O_3 system. Other prominent advantages of PM technique include the possibility of close control over the gradient composition and the net or near net shape forming of the structural materials. Since the Ni and Al_2O_3 precursors are in the form of powders, maximising the exposed surface area for the reaction, thus result in faster reaction and ensure higher percentage of materials to react [1]. The constituent powders nickel (Bendosen) and alumina (Sigma Aldrich) were collected. The size of Ni particles in the range of 10-30 μm and predominantly round in shapes. Al_2O_3 particles have irregular shapes and the size in the range of 50-70 μm. A set of layer mixtures for a 6-layered sample was prepared (100wt.%Ni, 20wt.%Al_2O_3+80wt.%Ni, 40wt.%Al_2O_3+60wt.%Ni, 60wt.%Al_2O_3+40wt.%Ni, 80wt.%Al_2O_3+20wt.%Ni, 100wt.%Al_2O_3) according to the molecular weight of nickel and alumina constituents. After blending, the powder mixtures were sieved through a 100 μm mesh. After that, the mixtures were dried in a vacuum oven. The stacking up process of the powder layers was carried out in a cylindrical steel die of 30 mm diameter according to the arrangement as shown in Figure 1(a).

The powder layers were then compacted using a hydraulic press under a load of 30 ton. After that, the green compact underwent through a heat treatment process to densify the sample using pressureless sintering technique. The sintering was carried out in a tube furnace (Elite Thermal Systems Limited) in argon atmosphere, following the two-step sintering profile as depicted in Figure 1(b) below. The sintering process includes a preheating stage of 30 minutes at 150ºC for the removal of moisture and chemical impurities from the sample. After that, a heating rate of 4°C/min was applied to reach the temperature 1200°C and holding time 3 hours was maintained at this sintering temperature. Finally, a cooling rate of 2°C/min was maintained to allow the specimen to cool down to room temperature.

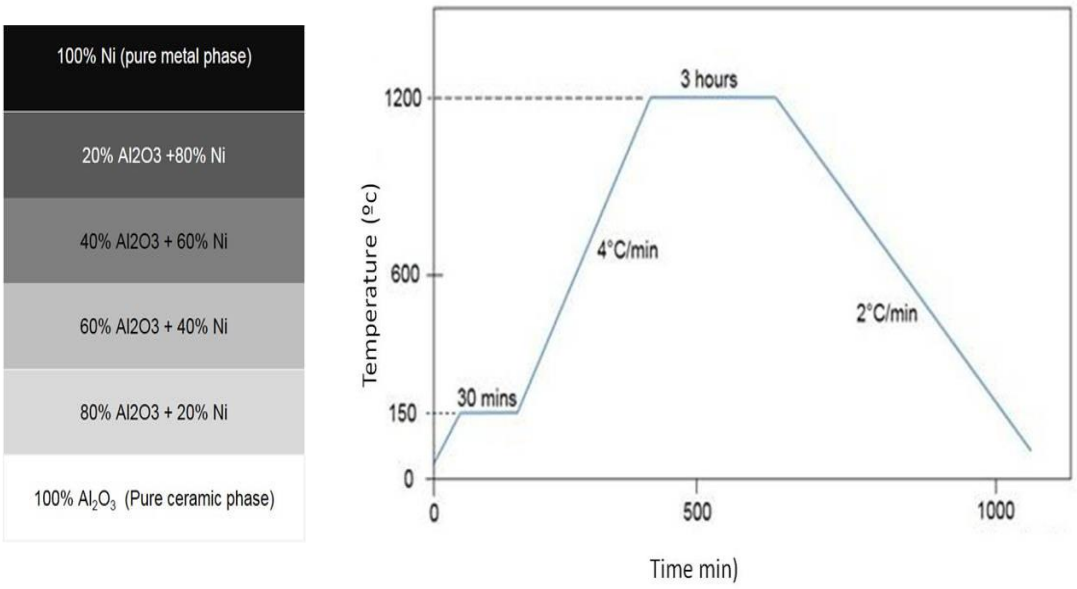

(a) (b)

Figure 1. (a) Illustration of layer arrangement for a 6-layered stepwise-built Ni-Al_2O_3 FGM sample (b) Two-step sintering cycle.

After sintering, the sintered samples were cut, ground and polished to prepare for microstructural characterization and hardness testing. Prepared samples were observed for microstructural characterization under metallurgical microscope (OLYMPUS BX51M). The hardness of individual layer was measured along the sample thickness using Vickers' microhardness tester (Wilson Hardness: Model 402 MD) under a 1 kgf (1 kN) load for dwell time of 15 seconds. Seven measurements of hardness were taken to ensure consistency and the average value was taken into consideration.

3. Results and Discussion

3.1. Densification and shrinkage

After the sintering process of the samples, it was believed that the samples were experienced shrinkage due to the formation of nickel-alumina bonding, hence the decrease of gaps between particles of constituent powders. Figure 2 compares the green compact and sintered samples. The sintered sample was viewed from the front and was seen clearly having a slanted shape along the sides in which the diameter at the top side (nickel) was larger than the diameter at the bottom side (alumina). The radial shrinkage of Ni/Al_2O_3 FGM samples was quantified by measuring the diameter of the green and sintered samples. Three average measurements had been recorded along the thickness for each specimen which were from top (0wt.% alumina), middle (60wt.% alumina) and bottom (100wt.% alumina) position. The measurements were taken from three different samples for consistency of results.

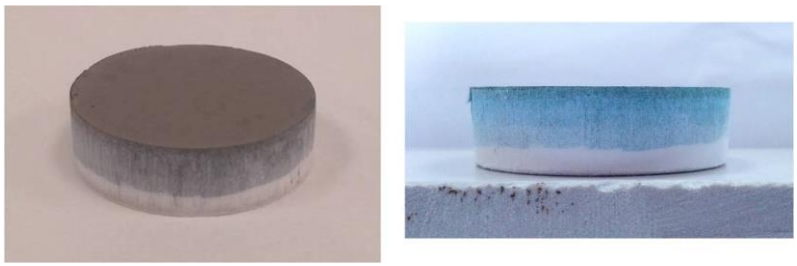

(a) (b)

Figure 2. Samples of 6-layered Ni/Al_2O_3 FGM (a) Green compact and (b) Sintered sample.

Figure 3 compares the diameter of the samples during pre and post sintering process. It can be seen that at pure nickel layer, there was a slight increase in diameter after sintering due to expansion of nickel in the radial direction. From the graph it is apparent that the diameter was shrunk with the increase in alumina wt.%. Larger shrinkage within the ceramic phase proves that during sintering, more porosities in the layer were eliminated.

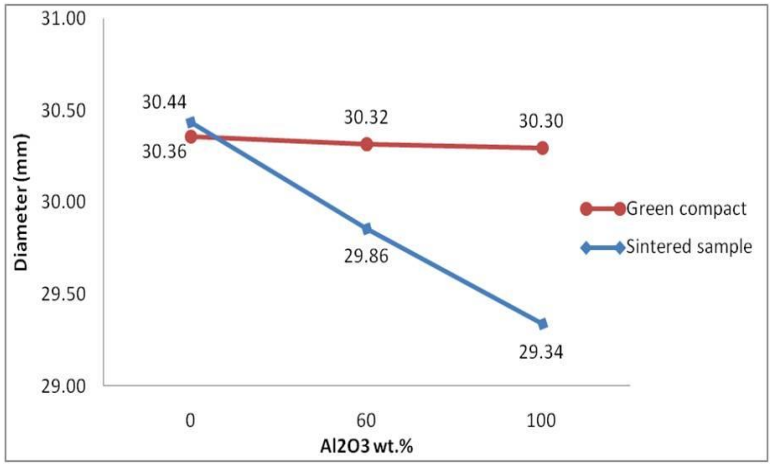

Figure 3. Distribution of diameter along the thickness for green and sintered specimens.

3.2. Microstructural analysis

Figures 4(a)-(f) show the optical micrographs of layers of different compositions for the 6-layered FG samples. In the following micrographs, at pure nickel and higher nickel composition layers, the metal particles (Ni) are revealed by the shiny and bright parts while ceramic constituents are represented by darker regions. On the other hand, at ceramic-dominant layers, Al_2O_3 constituents become more visible due to the lighting adjustment. At 80wt.% Ni composition, the volume part of nickel phase containing interconnected metal particles prevails over the alumina parts and forms the matrix phase. As the composition of alumina is increasing, metal interconnection decreased and the volume of nickel parts isolated between the ceramic constituents become more prevalent and viewed as the reinforcement phases. In the 60wt.% Ni layer, the interconnected nickel phases become isolated whereas alumina phase begin to combine and form clusters. In terms of the particle distribution, it can be referred from the micrographs of 80wt.% Ni layer that alumina particles are almost uniformly distributed in nickel matrix, so as nickel particles in the ceramic matrix of alumina-dominant layers (20wt.% and 40wt.% Ni layers).

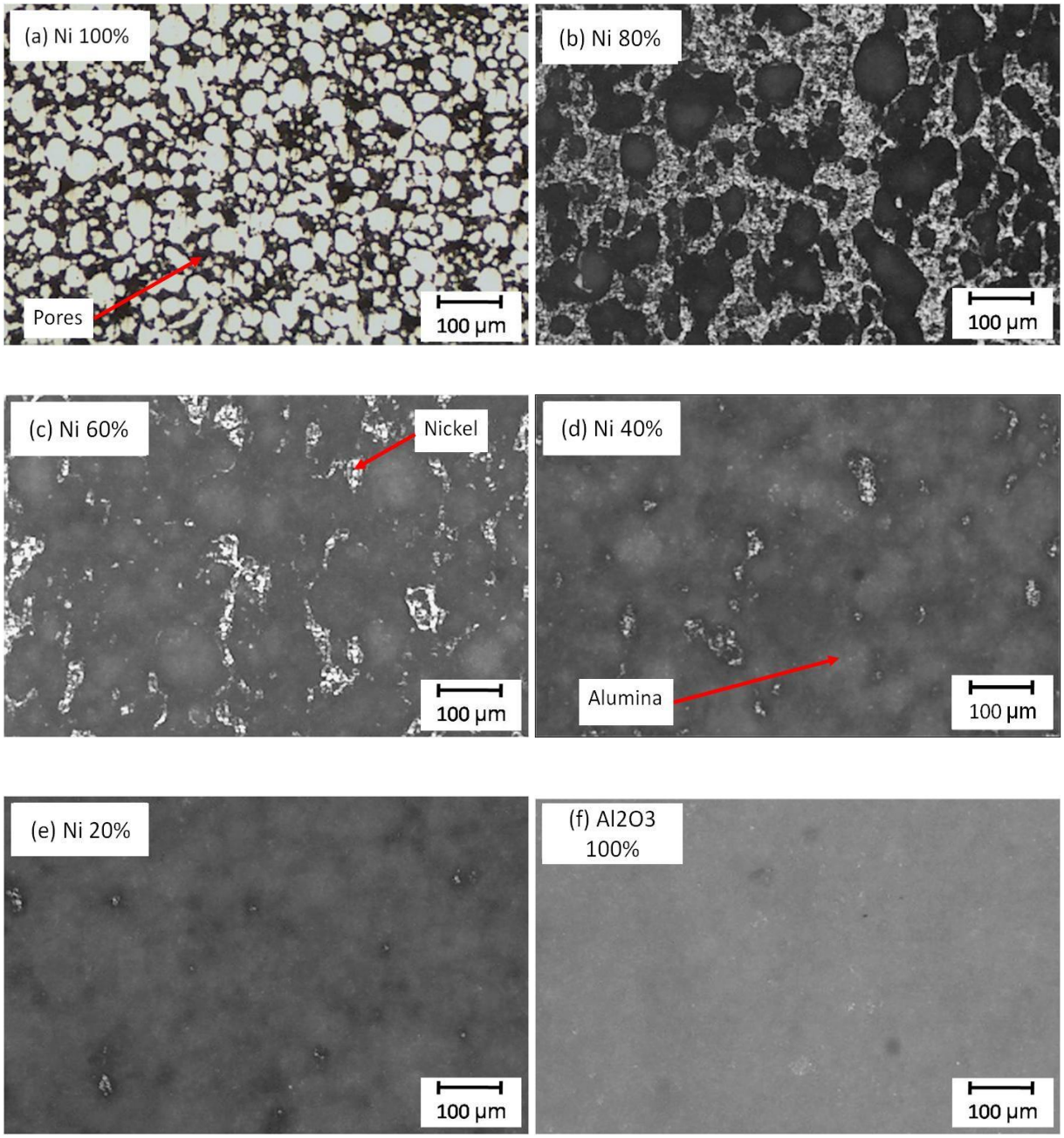

Figure 4. Micrographs of individual layers for 6-layered samples (a) 100wt.% Ni (b) 80wt.% Ni (c) 60wt.% Ni (d) 40wt.% Ni (c) 20wt.% Ni (d) 100wt.% Al_2O_3.

Figures 5(a)-(e) show the interfacial lines of 6-layered Ni/Al_2O_3 FGM. The existences of six layer compositions inside the FGM samples are confirmed from the difference in phase composition of adjacent layers and interfacial barriers. In general, it can be seen that all interfaces show a smooth transition in microstructure from one layer to the next and no crack was found along the interfaces. This confirms a good interfacial solid state bonding between metal-ceramic constituents and proper stacking process. The interface lines represented by dashed lines are almost straight and parallel (judging from the positions of the arrows on both sides of each micrograph which have close gaps) but also wavy at some localized area which indicates non-uniformity in the layer thickness as powders were stacked before compaction. However for 60wt.% Ni and 40wt.% Ni layer combination, the interface is less obvious and little difficult to recognize.

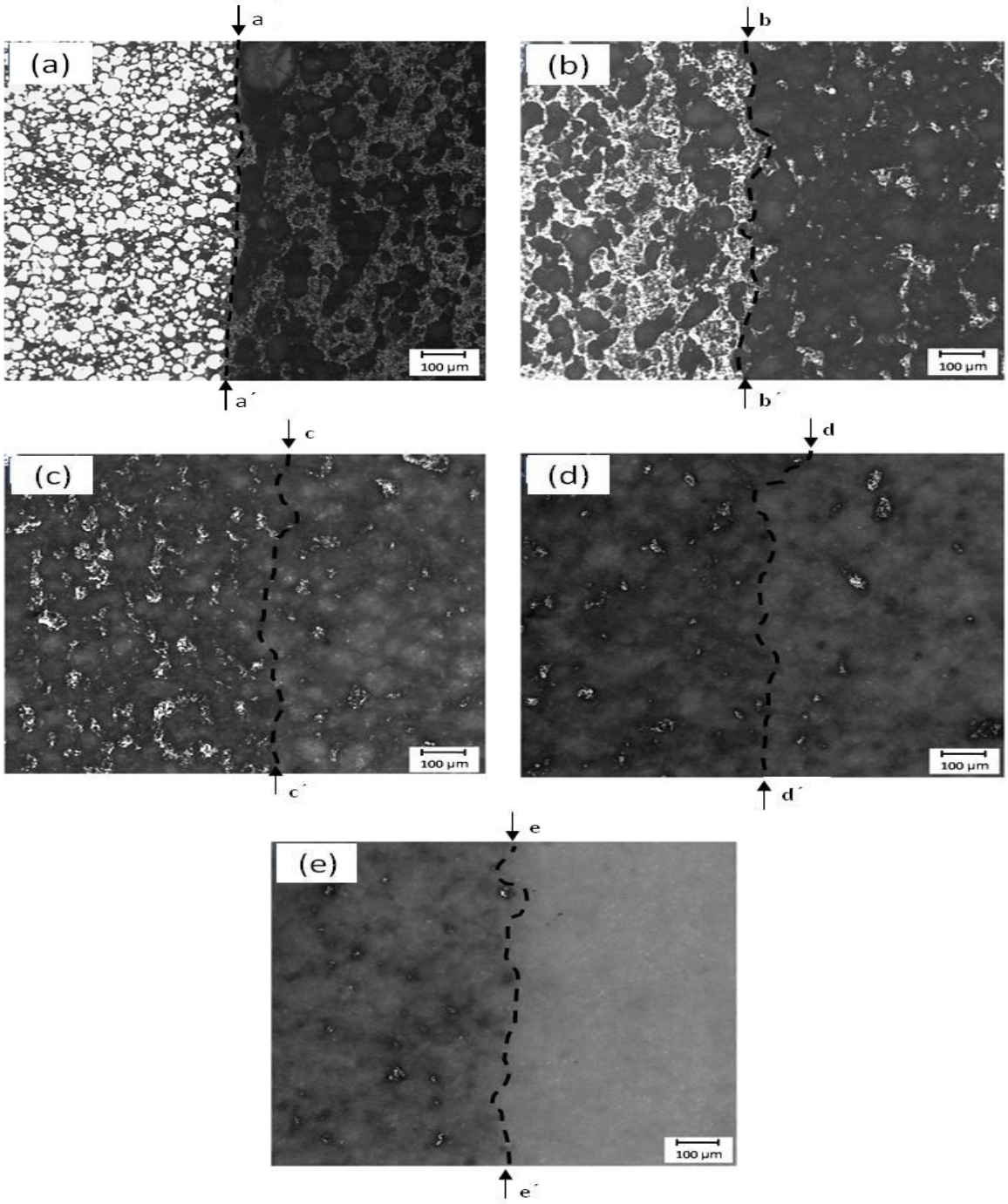

Figure 5. Interface lines of 6-layered Ni/Al_2O_3 FGM. (a) interface aa´ between 100wt.% Ni and 80wt.% Ni layers (b) interface bb´ between 80wt.% Ni and 60wt.% Ni layers (c) interface cc´ between 60wt.% Ni and 40wt.% Ni layers (d) interface dd´ between 40wt.% Ni and 20wt.% Ni layers (e) interface ee´ between 20wt.% Ni and 100wt.% Al_2O_3 layers.

3.3. Microhardness measurement

Figure 6 shows the variation in microhardness values across different layers. The microhardness in the Ni/Al_2O_3 FGM sample was measured at each distinctive layer to observe the hardness variation across the thickness direction. Seven hardness values at different locations were measured for each layer and the average value was taken into consideration. These results are plotted in the figure 6. The highest hardness was recorded on the pure nickel layer which is 150.00 HV while the lowest was at pure Al_2O_3 layer, 12.03 HV. The averaged plotted values show a slight decrease from pure Ni layer to 20 wt.% Al_2O_3 layer. From the obtained hardness values, the trend line implies that as the percentage of

Al_2O_3 composition increases, the microhardness values decrease. The hardness trends are contrary to the expected values and it is believed that sintering temperature and holding time are responsible for the incomplete transformation of Al_2O_3 particles into hard ceramic. This might also relate to the texture of alumina layer after sintering which is not very strong and eroded along the edge. This erosion of alumina is shown in Figure 7. The obtained results suggest that there might be increasing percentage of porosities in the FG structure as the ceramic content rises.

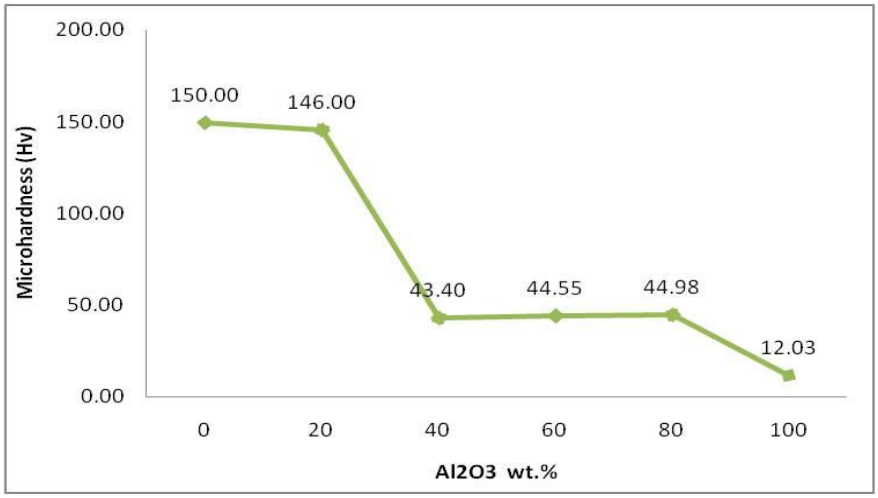

Figure 6. Variation in microhardness values across different layers for sample sintered for 3 hours.

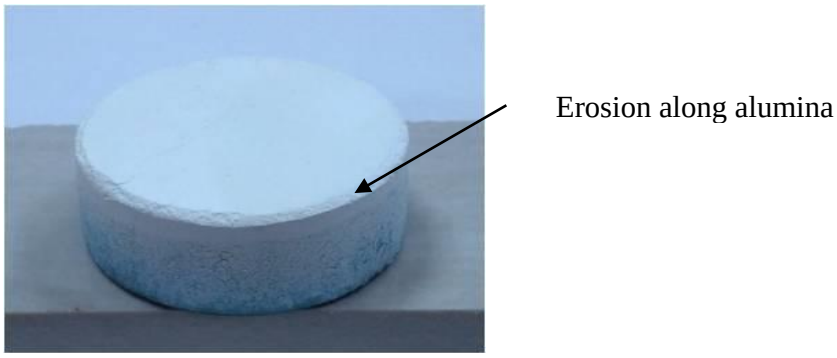

Figure 7. Alumina layer eroded on the edge.

4. Conclusion

Six-layered Ni-Al_2O_3 functionally graded composite materials were prepared through powder metallurgy and pressureless sintering technique. Two-step sintering cycle was applied in a tube furnace at sintering temperature of 1200ºC and sintering time of 3 hours. The obtained results revealed that in the ceramic rich layers, larger shrinkage occurred and more porosities were eliminated. Microstructural analyses showed that alumina particles are almost uniformly distributed in nickel matrix and nickel particles are also uniformly distributed in the alumina rich layers. From the interfacial analyses, it was observed that smooth transition of microstructure occurred from one layer to the next layer which confirms a good interfacial solid-state bonding. Microhardness test results suggest that alumina powders might not have sintered completely to transform into hard ceramic and it is believed that there is an increasing amount of micropores/microvoids in the graded structure as the ceramic content rises.

References

[1] EL-Wazery M S, EL-Desouky A R, Hamed O A, Fathy A and Mansour N A 2013 Electrical and mechanical performance of zirconia-nickel functionally graded materials *Int. J. Eng. Trans. A: Basics* **26** 375–82

[2] Khoddami A M, Sabour A and Hadavi S M M 2007 Microstructure formation in thermally sprayed duplex and functionally graded NiCrAlY/Yttria-stabilized zirconia coatings *Surf. Coat. Technol.* **201** 6019–24

[3] Rubio W M, Paulino G H and Silva E C N 2012 Analysis, manufacture and characterization of Ni/Cu functionally graded structures *Mater. Des.* **41** 255-6

[4] Wu K, Scheler S, Park H S and Porada M W 2013 Pressureless sintering of ZrO_2-$ZrSiO_4$/NiCr functionally graded materials with a shrinkage matching process *J. Eur. Ceram. Soc.* **33** 1111–21

[5] Watanabe Y, Hattori Y and Sato H 2015 Distribution of microstructure and cooling rate in Al-Al_2Cu functionally graded materials fabricated by a centrifugal method *J. Mater. Process. Technol.* **221** 197–204

[6] Shahrjerdi A, Mustapha F, Bayat M, Sapuan S M and Majid D L A 2011 Fabrication of functionally graded hydroxyapatite-titanium by applying optimal sintering procedure and powder metallurgy *Int. J. Phys. Sci.* **6** 2258–67

[7] Latiff M I A, Jamaludin S N S, Basri S, Hussain A, Al-Othmany D S, Mustapha F, Nuruzzaman D M, Ismail N M and Ismail I 2014 Effect of sintering temperature on functionally graded nickel/alumina plate *Appl. Mech. Mater.* **629** 437-43

[8] Sun L, Sneller A and Kwon P 2008 Fabrication of alumina/zirconia functionally graded material: from optimization of processing parameters to phenomenological constitutive model *Mater. Sci. Eng. A* **488** 31–8

[9] Bhattacharyya M, Kumar A N and Kapuria S 2008 Synthesis and characterization of Al/SiC and Ni/Al_2O_3 functionally graded materials *Mater. Sci. Eng. A* **487** 524-35

[10] Hosseini S S, Bayesteh H and Mohammadi S 2013 Thermo-mechanical XFEM crack propagation analysis of functionally graded materials, *Mater. Sci. Eng. A* **561** 285-302

[11] Tahvilian L and Fang Z Z 2012 An investigation on thermal residual stresses in a cylindrical functionally graded WC-Co component *Mater. Sci. Eng. A* **557** 106-12

[12] Jamaludin S N S, Basri S, Hussain A, Al-Othmany D S, Mustapha F and Nuruzzaman D M 2014 Three-dimensional finite element modeling of thermomechanical problems in functionally graded hydroxyapatite/titanium plate *Math. Probl. Eng.* **2014** 1-20

[13] Erdemir F, Canakci A and Varol T 2015 Microstructural characterization and mechanical properties of functionally graded Al2024/SiC composites prepared by powder metallurgy techniques *Trans. Nonferrous Met. Soc. China* **25** 3569-77

[14] Radhika N and Raghu R 2016 Development of functionally graded aluminium composites using centrifugal casting and influence of reinforcements on mechanical and wear properties *Trans. Nonferr. Met. Soc. China* **26** 905-16

[15] Jamaludin S N S, Basri S, Mustapha F, Nuruzzaman D M, Latiff M I A and Ismail N M 2017 Phase contamination characterization of stepwise-bulit functionally graded hydroxyapatite/titanium (HA/Ti) sintered under various atmospheres *Mater. Sci. Forum* **889** 90–5

[16] Zhang C H, Zhang H, Wu C L, Zhang S, Sun Z L and Dong S Y 2017 Multi-layer functional graded stainless steel fabricated by laser melting deposition *Vacuum* **141** 181-7